NACA TN 3895

NATIONAL ADVISORY COMMITTEE
FOR AERONAUTICS

TECHNICAL NOTE 3895

OBLIQUE-SHOCK RELATIONS AT HYPERSONIC SPEEDS

FOR AIR IN CHEMICAL EQUILIBRIUM

By W. E. Moeckel

Lewis Flight Propulsion Laboratory
Cleveland, Ohio

NACA

Washington

January 1957

NATIONAL ADVISORY COMMITTEE FOR AERONAUTICS

TECHNICAL NOTE 3895

OBLIQUE-SHOCK RELATIONS AT HYPERSONIC SPEEDS

FOR AIR IN CHEMICAL EQUILIBRIUM

By W. E. Moeckel

SUMMARY

Oblique-shock relations for air in chemical equilibrium have been calculated for flight velocities up to 25,000 feet per second at altitudes up to 200,000 feet. Results show that those shock parameters which are functions only of Mach number normal to the shock for an ideal gas are strongly influenced by flight altitude (initial conditions), as well as normal Mach number, when dissociation takes place.

The variation of flow-deflection angle with shock angle differs significantly from that of an ideal gas. At an altitude of 100,000 feet and a flight speed of 25,000 feet per second, for example, the wedge detachment angle is about 14° larger than that obtained for an ideal gas.

INTRODUCTION

Tables and charts of oblique-shock relations for air are currently available only for downstream temperatures less than 5000° R (ref. 1). Recent computations by the National Bureau of Standards of the properties of air in chemical equilibrium at temperatures up to 15,000° K (ref. 2) permit extension of these charts to the regions of interest for hypersonic aerodynamics of nonslender bodies. Some representative computations, based on the data of reference 2, have recently been completed at the NACA Lewis Laboratory and are reported herein. Although these computations are not as detailed as those of reference 1, they contain sufficient information to calculate with reasonable accuracy the inviscid flow quantities downstream of oblique shocks of arbitrary strength for flight speeds up to 25,000 feet per second and altitudes up to 200,000 feet. The principal limitation in the use of the oblique-shock relations presented herein is the assumption that the air is in equilibrium downstream of the shock.

Two evaluations of shock relations for air in equilibrium have been published recently (refs. 3 and 4). Both references are limited to normal-shock relations. Reference 3 was published before thermodynamic

data based on the corrected dissociation energy of nitrogen (9.76 electron volts) became available. Reference 4 uses the corrected thermodynamic data and compares results with the values obtained with the previously accepted nitrogen dissociation energy of 7.37 electron volts.

ANALYSIS

In the nomenclature shown in the following sketch, the equations of
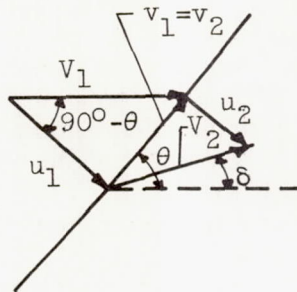
continuity, conservation of momentum, conservation of energy, and state are as follows:

$$\rho_2 u_2 = \rho_1 u_1 \tag{1}$$

$$g(p_2 - p_1) = \rho_1 u_1^2 - \rho_2 u_2^2 \tag{2a}$$

$$v_2 = v_1 \tag{2b}$$

$$2gJ(h_2 - h_1) = u_1^2 - u_2^2 \tag{3}$$

$$p_2 = RJ \frac{\rho_2 t_2}{m_2} \tag{4}$$

All symbols are defined in the appendix.

Equations (1) and (2a) yield the following expression for a pressure coefficient based on normal Mach number $M_1 \sin \theta$:

$$\frac{\dfrac{p_2}{p_1} - 1}{\gamma_1 M_1^2 \sin^2\theta} = 1 - \frac{u_2}{u_1} \tag{5}$$

Equation (3) can be put into the form of an enthalpy coefficient based on normal Mach number as follows:

$$\frac{\dfrac{h_2}{h_1} - 1}{\dfrac{\gamma_1 - 1}{2} M_1^2 \sin^2\theta} = 1 - \left(\frac{u_2}{u_1}\right)^2 \tag{6}$$

In equation (6) it is assumed that ambient temperature is low enough that the following ideal-gas relations hold: $h_1 = c_{p,1} t_1$ and $\gamma_1 = \dfrac{c_{p,1}}{c_{v,1}}$.

The relation between flow-deflection angle δ and shock angle θ can be expressed as

$$\tan(\theta - \delta) = \frac{u_2}{v_2} = \frac{u_2}{v_1} = \frac{u_2}{u_1}\frac{u_1}{v_1} = \frac{u_2}{u_1}\tan\theta$$

or

$$\frac{\tan(\theta - \delta)}{\tan\theta} = \frac{u_2}{u_1} \tag{7}$$

Equations (5), (6), and (7) show that all quantities downstream of the shock (except the speed of sound) can be determined if the ratio of normal-velocity components across the shock u_2/u_1 is known. For, with p_2 and h_2 known, the other state quantities ρ_2, t_2, and m_2 can be obtained from the computed properties of air in equilibrium presented in reference 2. The determination of these state relations is greatly simplified by use of thermodynamic charts for air prepared from the data of reference 2.

The procedure used to solve for u_2/u_1 was as follows:

(1) Compute p_2 and h_2 from equations (5) and (6), respectively, for several assumed values of u_2/u_1 near the expected correct value.

(2) With the values of p_2 and h_2, use thermodynamic charts to obtain t_2 and m_2. Compute ρ_2 from equation (4).

(3) Plot ρ_2/ρ_1 from step (2) against assumed u_1/u_2 values. The point of intersection of this curve with the line $\rho_2/\rho_1 = u_1/u_2$ yields the correct value of u_2/u_1.

Speed of sound downstream of shock. - The speed of sound of a gas in equilibrium is given by

$$a^2 = g\left(\frac{\partial p}{\partial \rho}\right)_S \tag{8}$$

where the subscript S indicates that the derivative is taken along an isentrope. Alternatively, the speed of sound can be expressed by

$$a^2 = \frac{\gamma g p}{\rho} = \frac{\gamma g J R t}{m} \tag{9}$$

where γ is the local isentropic exponent[1], which is given by

$$\gamma = \left(\frac{\partial \log p}{\partial \log \rho}\right)_S \tag{10}$$

From the equation of state, the following equivalent formulas are derived:

$$\left(\frac{d \log p}{d \log \frac{t}{m}}\right)_S = \frac{\gamma}{\gamma - 1} \tag{11}$$

and

$$\left(\frac{d \log \rho}{d \log \frac{t}{m}}\right)_S = \frac{1}{\gamma - 1} \tag{12}$$

The variations of $\log p$ and $\log \rho$ with $\log \frac{t}{m}$ along isentropes were obtained from thermodynamic charts plotted from the data of reference 2 and from the equation of state. Values of γ were then obtained from equations (11) and (12) by measuring the local slopes of these curves. Results are shown as a function of enthalpy in figure 1 for several values of S/R_0. Although some interpolation error is involved in reading the thermodynamic charts, the values of γ obtained from equations (11) and (12) agreed within ± 0.02.

With γ known, the speed of sound is calculated from equation (9) after p and ρ are determined.

------

[1]The isentropic exponent is, of course, not equal to the ratio of specific heats when dissociation takes place. Definition of γ as in eq. (10) avoids the necessity of calculating specific heats for the dissociating gas.

RESULTS

Computations were carried out for the following combinations of ini-
tial velocity and altitude:

Altitude, ft	Initial velocity, V_1, ft/sec
100,000	5,000 10,000 15,000 20,000 25,000
50,000 150,000 }	{ 5,000 15,000 25,000
200,000	25,000

The ambient conditions used at each altitude are given in table I.

The computations are simplified considerably if it is noted that
u_2/u_1 is, for given initial conditions, a function only of the normal
Mach number $M_1 \sin \theta$. (In general, if the initial enthalpy is suffi-
ciently large that h_1 cannot be set equal to $c_{p,1}t_1$, then u_2/u_1 is
a function of the initial normal velocity u_1 instead of $M_1 \sin \theta$.)
Consequently, the pressure ratio and enthalpy ratio for given initial
conditions are also functions only of $M_1 \sin \theta$. Since h_2 and p_2
determine S_2, t_2, m_2, and ρ_2, these quantities are also functions only
of $M_1 \sin \theta$.

Normal-Velocity Ratio u_2/u_1

The ratio u_2/u_1 is plotted in figure 2 as a function of the normal
Mach number $M_1 \sin \theta$. Shown for comparison is the variation obtained
from the constant γ formula:

$$\frac{u_2}{u_1} = \frac{\gamma - 1}{\gamma + 1} \left(1 + \frac{1}{\frac{\gamma - 1}{2} M_1^2 \sin^2\theta} \right) \tag{13}$$

For normal Mach numbers less than 4, the real-gas results differ little from the $\gamma = 1.4$ values. In the range of normal Mach numbers from 4 to 25, the dissociation of air becomes more and more significant, and the normal-velocity ratio approaches the $\gamma = 1.15$ curve. The effect of altitude (initial temperature and pressure) is quite appreciable. The initial divergence from the $\gamma = 1.4$ curve is due to oxygen dissociation. For $M_1 \sin \theta$ near 14, the oxygen is almost entirely dissociated, and the curves tend toward the horizontal. For somewhat larger values of $M_1 \sin \theta$, the dissociation of nitrogen becomes significant, and the curves again move downward.

Flow Deflection Across Shock

The relation between flow-deflection angle across the shock δ and shock angle θ is shown in figure 3(a) for an altitude of 100,000 feet. The constant γ curves, for $\gamma = 1.4$, seriously underestimate the deflection angle for shock angles greater than about 30° when the flight speed is greater than 5000 feet per second. The detachment angle, for example, is 60.1° for $V_1 = 25,000$ feet per second, as compared with 45.6° for infinite Mach number with $\gamma = 1.4$. The effect of altitude is shown in figure 3(b).

Mach Number Behind Shock

In figure 4, the Mach number downstream of the shock is plotted against shock angle for several flight speeds at an altitude of 100,000 feet. Of particular interest is the fact that the sonic point moves from $\theta = 67^\circ$ at 5000 feet per second to $\theta = 75^\circ$ at 25,000 feet per second. (For $\gamma = 1.4$, the sonic point is $\theta = 68^\circ$ for $M_1 = \infty$.)

Mass-Flow Ratio

The ratio of the mass flow per unit area across the shock $\rho_2 V_2 / \rho_1 V_1$ is shown in figure 5. This ratio is the reciprocal of the stream-tube-area ratio across the shock. The maximum mass-flow ratio occurs at shock angles considerably smaller than that at the sonic point. This result is due to the strong entropy change with shock angle and is also obtained using ideal-gas theory.

Temperature

The temperature downstream of the shock is shown in figure 6 as a function of normal Mach number. Temperatures are higher at 50,000 feet than at 100,000 feet because of the higher pressure at lower altitudes

which inhibits dissociation. The initially higher downstream temperatures at 150,000 feet are, of course, due to the higher ambient temperature at this altitude.

Entropy Increase

The increase in entropy across oblique-shock waves is shown in figure 7 as a function of normal Mach number. Considerably larger increases in entropy are obtained at high normal Mach numbers for the real gas than for the ideal gas.

Other Parameters

With the oblique-shock relations plotted in figures 2 to 7, all other flow parameters downstream of the shock are easily obtained. The density ratios across the shock are simply the reciprocals of the normal-velocity ratios of figure 2. Pressure and enthalpy downstream of the shock are also obtainable from figure 2 with the aid of equations (5) and (6). The absolute velocity and speed of sound downstream of the shock can be calculated from

$$V_2^2 = u_2^2 + V_1^2 \cos^2\theta \tag{14a}$$

or

$$V_2 = V_1 \left(\frac{\rho_2 V_2}{\rho_1 V_1}\right) \frac{u_2}{u_1} \tag{14b}$$

and

$$a_2 = \frac{V_2}{M_2} \tag{15}$$

where u_2/u_1 is obtained from figure 2, $\rho_2 V_2 / \rho_1 V_1$ from figure 5, and M_2 from figure 4.

Lewis Flight Propulsion Laboratory
    National Advisory Committee for Aeronautics
        Cleveland, Ohio, October 17, 1956

APPENDIX - SYMBOLS

a   speed of sound, ft/sec

c_p specific heat at constant pressure

c_v specific heat at constant volume

g   acceleration due to gravity, 32.16 ft/sec^2

h   enthalpy, Btu/lb (h = 0 for undissociated air at t = 0)

J   mechanical equivalent of heat, 778 ft-lb/Btu

M   Mach number

m   molecular weight, lb/lb-mole

m_0 molecular weight of undissociated air (28.86 for composition of ref. 2)

p   pressure, lb/sq ft

R   gas constant, 1.987 Btu/(lb-mole)($^\circ$R)

R_0 R/m_0

S   entropy, Btu/(lb)($^\circ$R)

t   temperature, $^\circ$R

t_0 reference temperature of reference 2, 491.69° R

u   velocity component normal to shock, ft/sec

V   resultant velocity, ft/sec

v   velocity component parallel to shock, ft/sec

γ isentropic exponent (γ_1 = 1.4)

δ flow-deflection angle across shock, deg

θ shock angle, deg

ρ density, lb/cu ft

Subscripts:

S   differentiation along isentrope

1   conditions upstream of shock

2   conditions downstream of shock

REFERENCES

1. Ames Research Staff: Equations, Tables, and Charts for Compressible
     Flow. NACA Rep. 1135, 1953. (Supersedes NACA TN 1428.)

2. Hilsenrath, Joseph, and Beckett, Charles W.: Thermodynamic Properties
     of Argon-Free Air $(0.78847N_2, 0.211530_2)$ to 15,000° K. Rep. 3991,
     U.S. Dept. Commerce, Nat. Bur. Standards, Apr. 1, 1955.

3. Squire, W., Hertzberg, A., and Smith, W. F.: Real Gas Effects in a
     Hypersonic Shock Tunnel. AECD-TN-55-14, Arnold Eng. Dev. Center,
     Air Res. and Dev. Command, Mar. 1955. (Contract No. AF 40(600)-6.)

4. Romig, Mary F.: The Normal Shock Properties of Air in Dissociation
     Equilibrium. Jour. Aero. Sci., vol. 23, no. 2, Feb. 1956, pp. 185-
     186.

TABLE I. - ASSUMED AMBIENT CONDITIONS

Altitude, ft	Pressure, p_1, atm	Density, ρ_1, lb/sq ft	Temperature, t_1, °R	Dimensionless enthalpy, $h_1/R_0 t_0$	Dimensionless entropy, S_1/R_0
0	1.0	0.0765	519	3.70	23.6
50,000	0.1145	0.01165	392.4	2.795	25.0
100,000	0.0106	0.001065	392.4	2.795	27.4
150,000	0.00142	9.81×10^{-5}	573.5	4.085	30.9
200,000	0.000314	1.988×10^{-5}	619.4	4.41	32.7
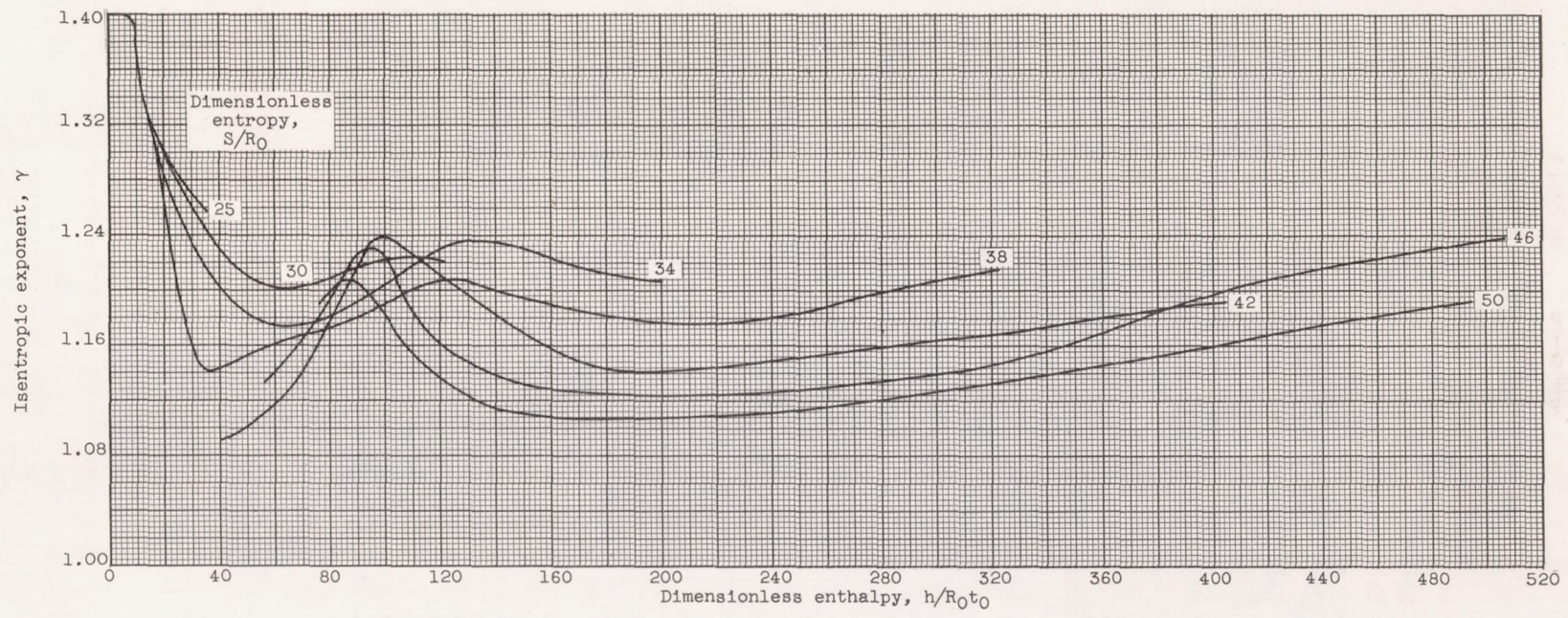
Figure 1. - Isentropic exponent for air in equilibrium.
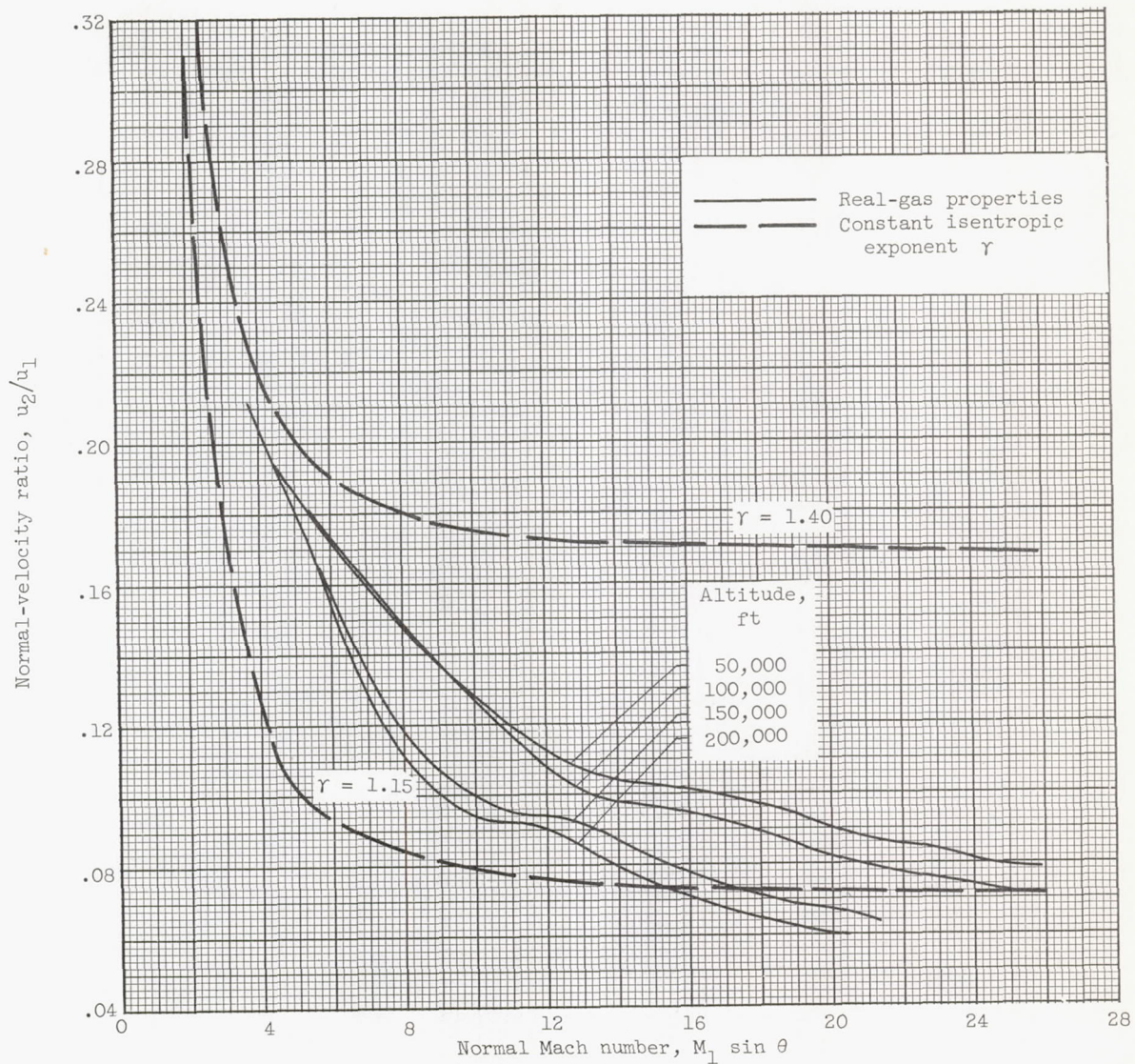
Figure 2. - Normal-velocity ratio across shock waves as function of normal Mach number.

4181
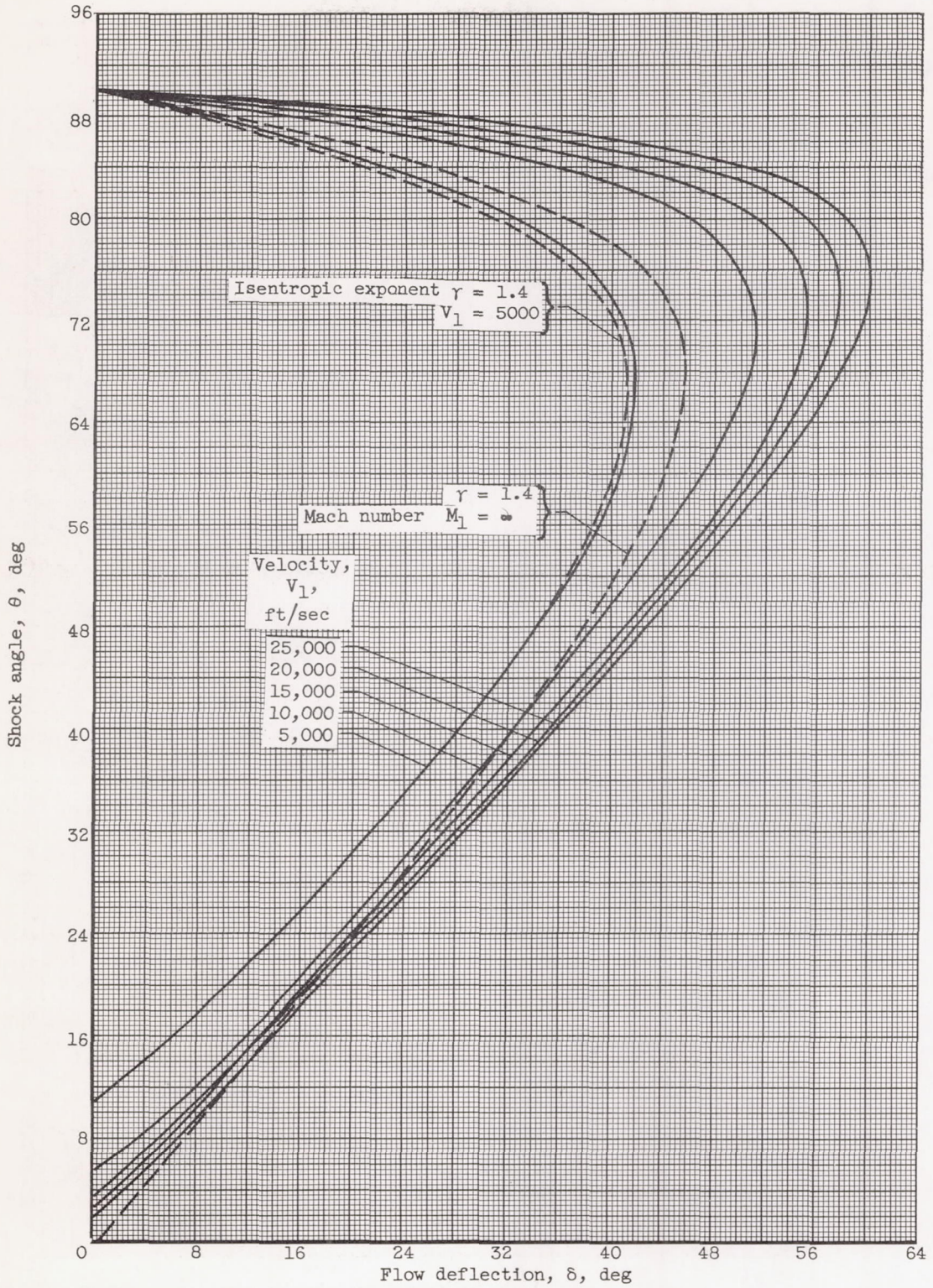
(a) Effect of velocity. Altitude, 100,000 feet.

Figure 3. - Shock angle as function of flow-deflection angle.
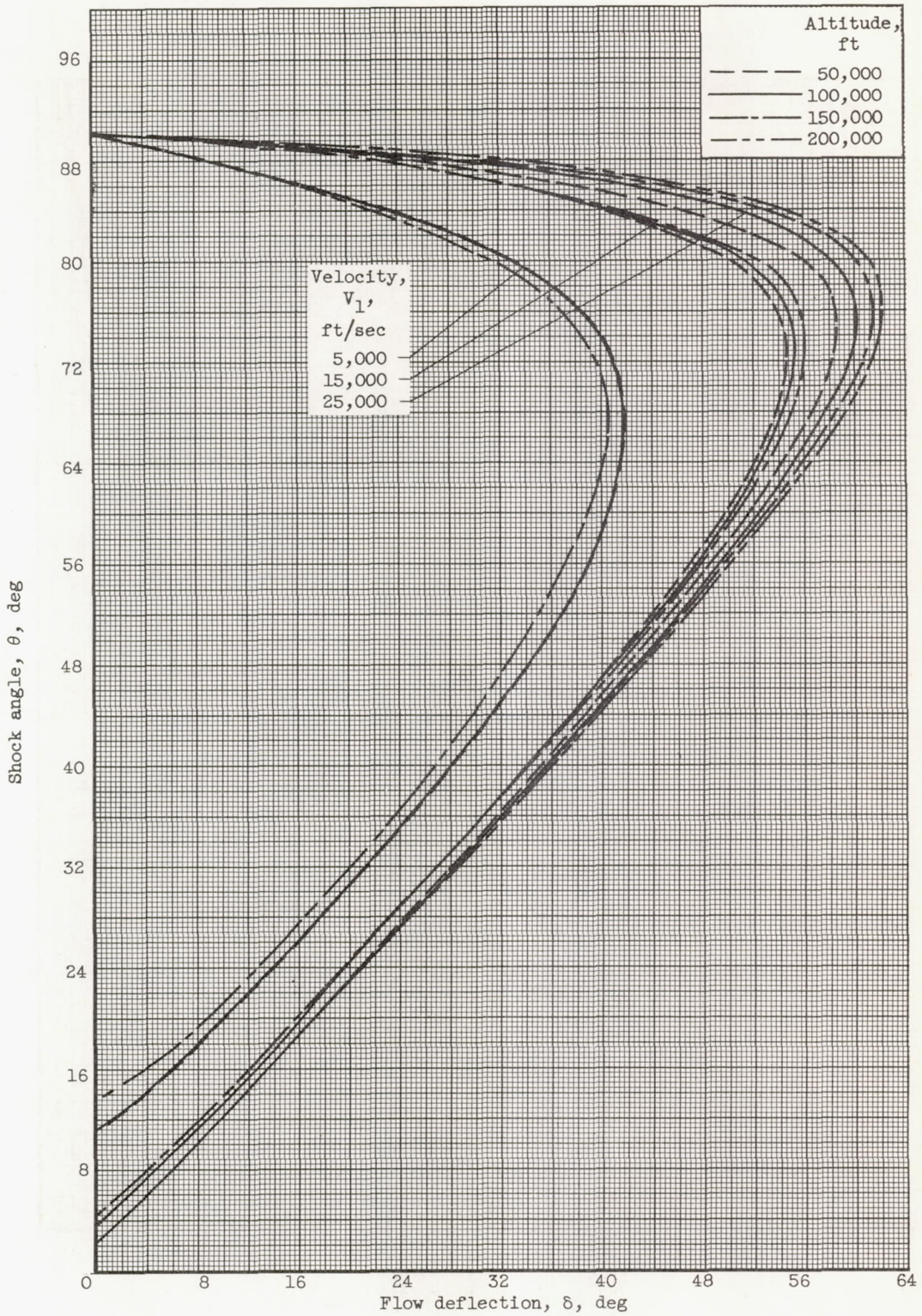
(b) Effect of velocity and altitude.

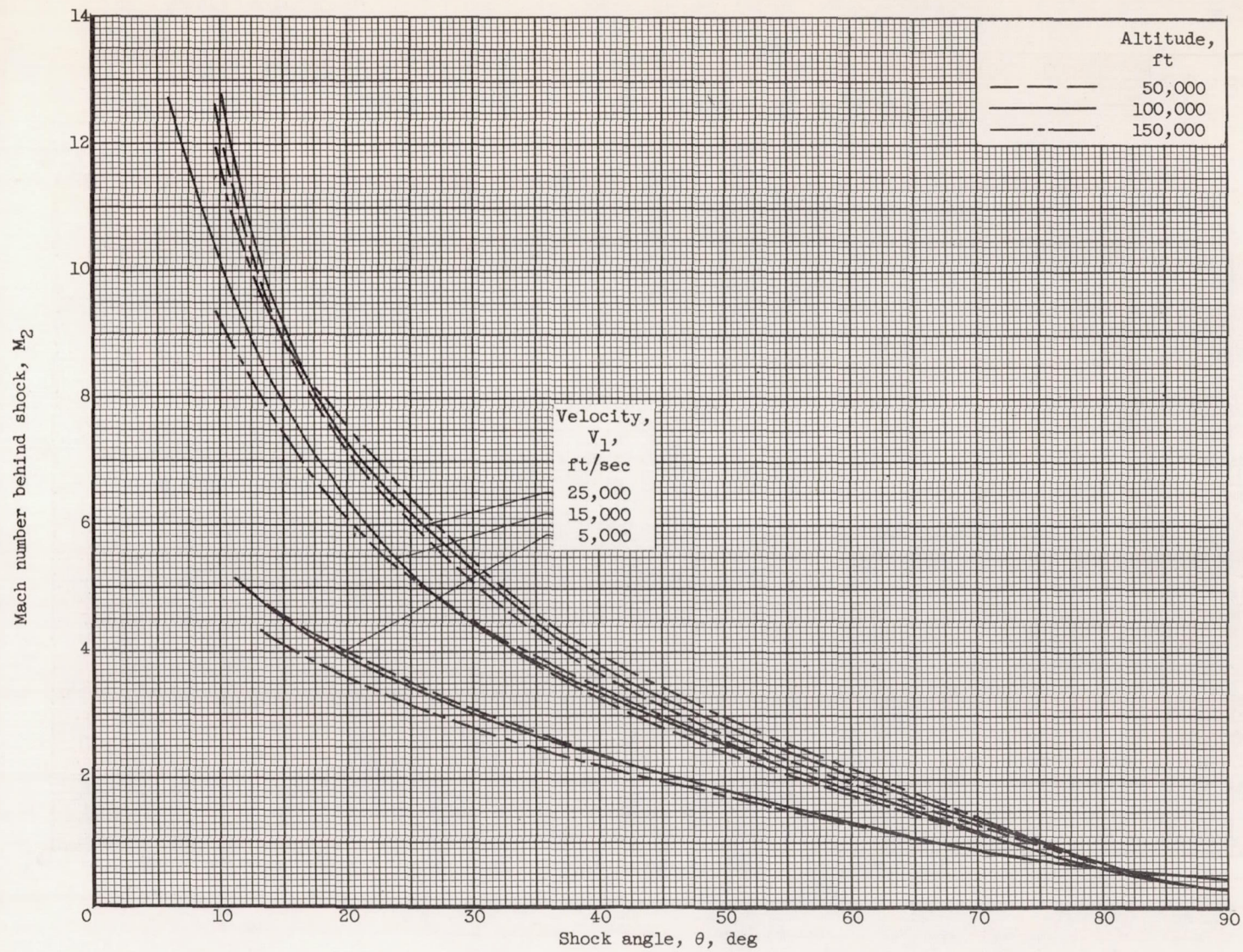Figure 3. - Concluded. Shock angle as function of flow-deflection angle.
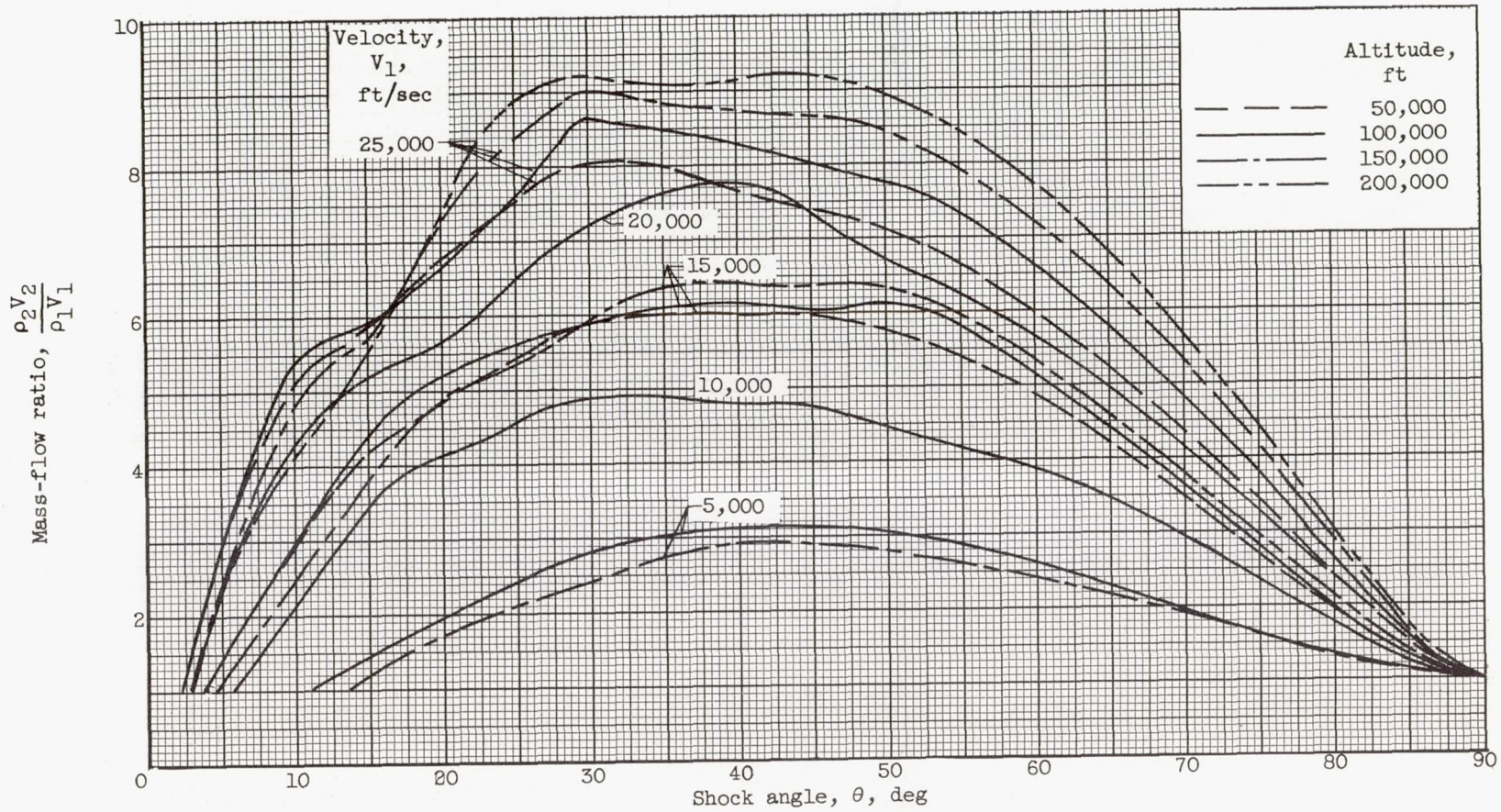
Figure 4. - Mach number downstream of shock.

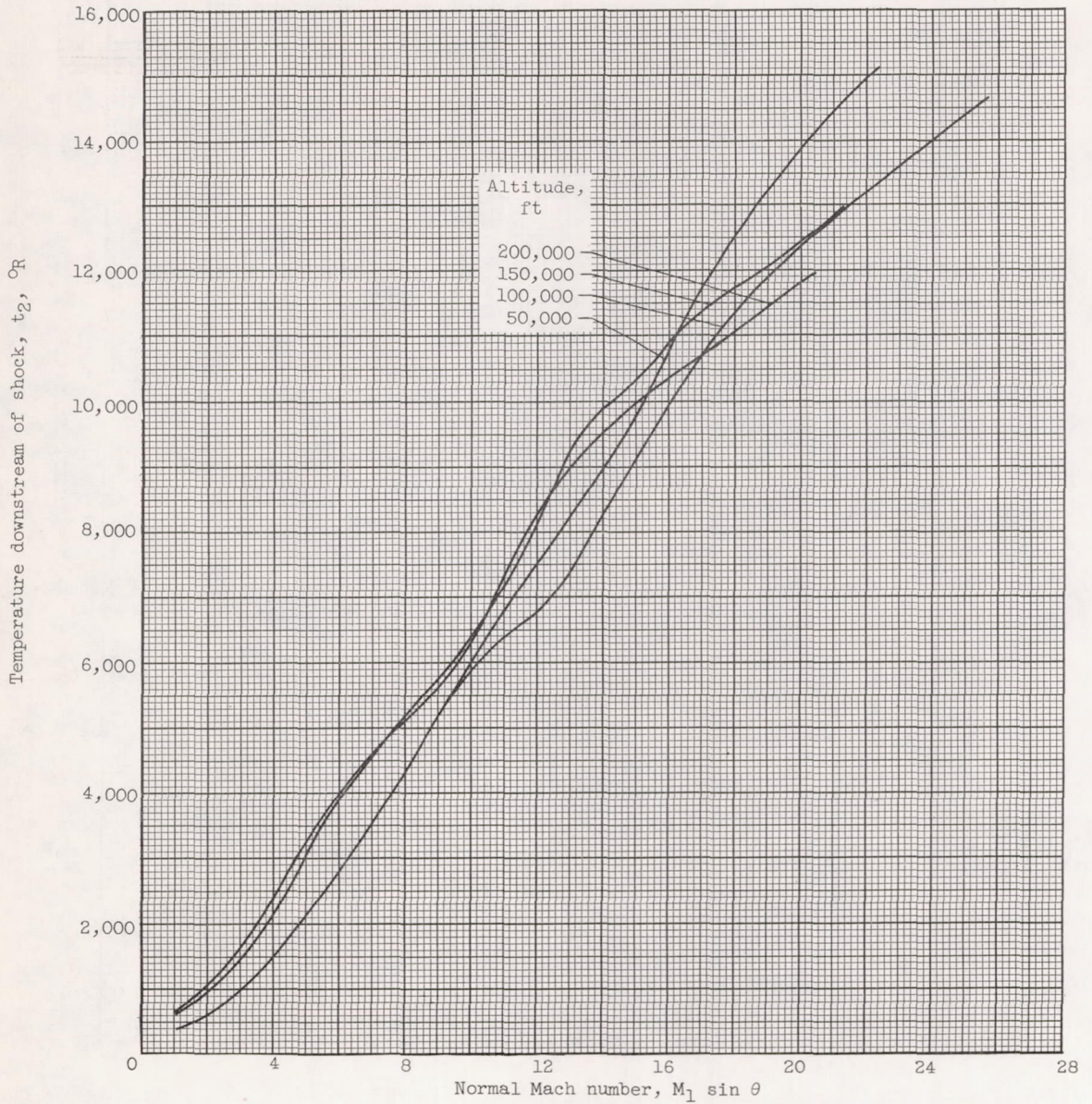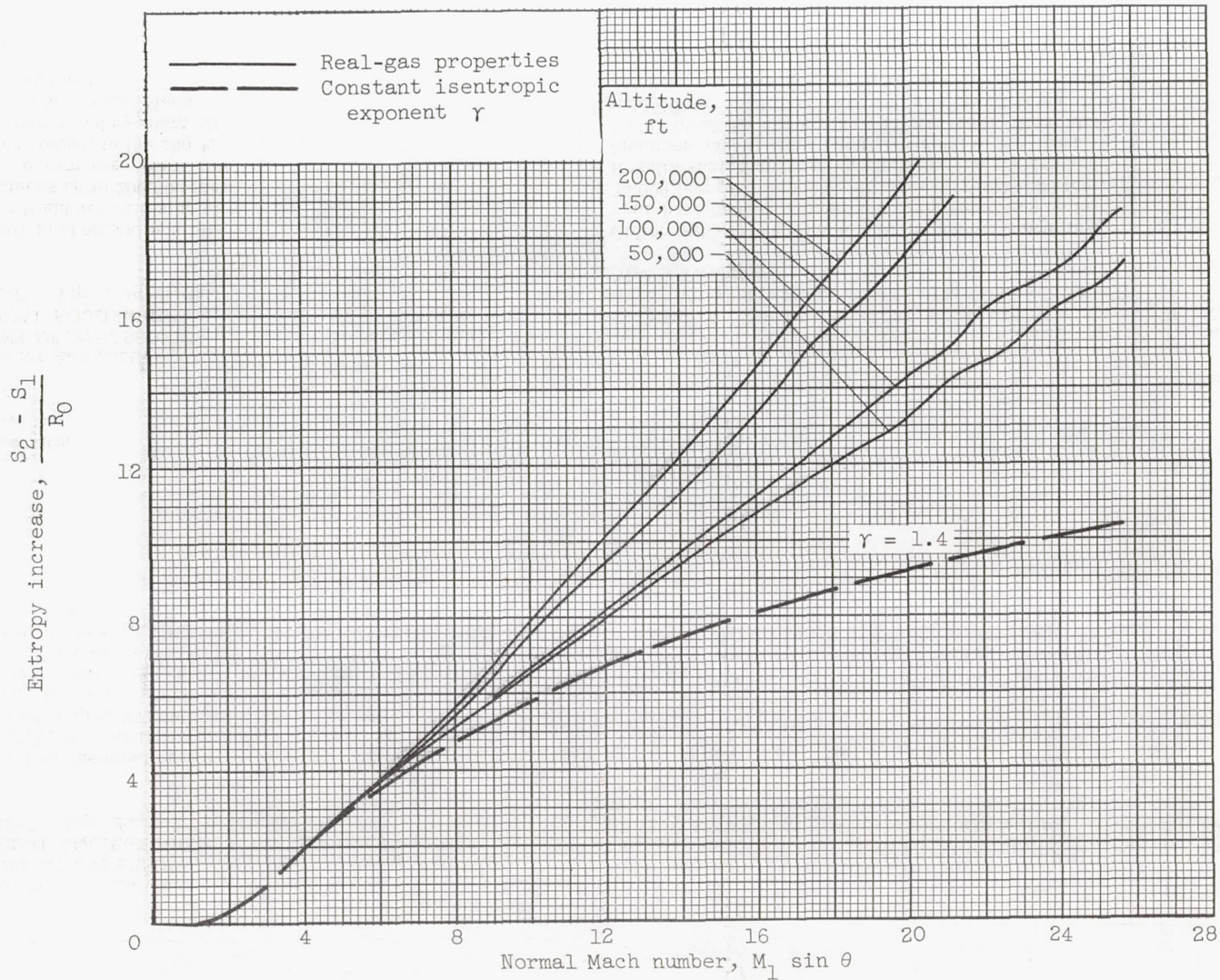Figure 5. - Mass-flow ratio across shock waves.

Figure 6. - Temperature downstream of shock wave.

Figure 7. - Entropy increase across shock waves.